Framework Topology of ERS-10 Zeolite**

Stefano Zanardi,* Giuseppe Cruciani, Luciano C. Carluccio, Giuseppe Bellussi, Carlo Perego, and Roberto Millini*

Dedicated to Professor Jens Weitkamp on the occasion of his 60th birthday

Zeolites are crystalline microporous aluminosilicates with frameworks based on a three-dimensional (3D) network of corner-sharing TO_4 (T = Si, Al) tetrahedra. A zeolite framework can be described as a regular assembly of finite (secondary building units, SBUs) or infinite building units (periodic building units, PerBUs). These PerBUs are layers or chains that stack in one or two directions according to given symmetry operations and/or simple lateral translations to build a regular 3D structure. However, when two or more stacking modes are possible, the same PerBU gives rise to different regular 3D structures, as well as to disordered intermediates arising from deviation of the stacking sequence from the periodic ordering. Ordered 3D structures (known as end-members) and disordered intermediates built with the same PerBU belong to the same family of structure types; the most notable examples are ZSM-11 and Beta zeolites. ZSM-11 is an intergrowth of MFI and MEL end-members of the pentasil family, which can be built by applying different symmetry operations to the same pentasil (PerBU) layer: inversion (*i*) in the case of MFI and reflection (*m*) in the case of MEL.[1]

Analogously, the structure of zeolite Beta can be described as an intergrowth of polymorphs stacked along the *c* direction.[2,3] The stacking faults are manifested by anisotropic broadening of a selected class of reflection peaks in powder diffraction patterns. According to Newsam et al.,[2] "The diffraction intensity from faulted complex materials can be computed by exploiting the recursive properties of faulting sequences in crystals". This approach was implemented in their program DIFFaX,[4] which is based on a recursion algorithm and allows simulation of X-ray diffraction patterns (XRD) from faulted materials.

Recently, Carluccio et al.[5] reported the synthesis of the new zeolite ERS-10 by using 6-azonia-spiro-[5,5]-undecane hydroxide as a structure-directing agent (SDA); the XRD pattern of ERS-10 is characterized by the features typical of an intergrowth material, namely the contemporaneous presence of sharp and broad reflections (Figure 1). These features

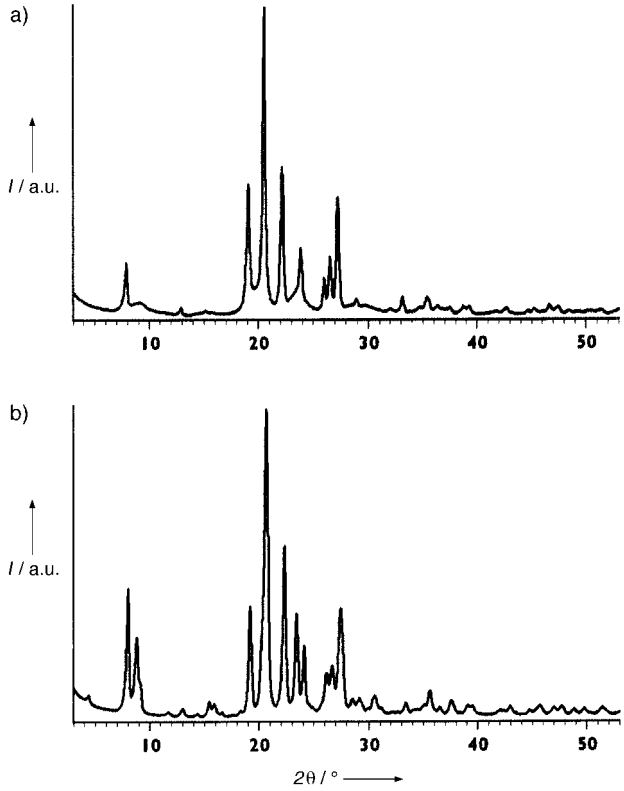

Figure 1. XRD patterns of a) as-synthesized ERS-10 and b) EUO.

make a structural characterization of this zeolite very difficult, requiring extensive model building of the stacking sequences and comparison of the DIFFaX computed patterns with the experimental one.

Preliminary structural characterization[6] indicated that the XRD pattern of ERS-10 is closely related to that of EU-1[7] (IZA code EUO) (Figure 1).

According to Marler and Gies,[8] EUO is in turn structurally related to two other zeolites: nonasil[8] (IZA code NON) and NU-87[9] (IZA code NES). Inspection of the unit cell parameters of these zeolites indicated that parameters *a* and *b* are very similar, while *c* varies in a regular way from NON to NES (Table 1). In fact, all these structures can be built from the same pseudo-hexagonal sheet defined by Briscoe et al. for EUO.[7] In all cases, the sheets regularly stack along the *c* axis and are interconnected by O atoms only in the case of NON; otherwise they are interconnected by O atoms and -O-Si-O-Si-O- bridges in EUO, and by -O-Si-O-Si-O- bridges in NES.[9] In the case of ERS-10, the sharp reflections present in the XRD pattern were indexed according to an orthorhombic unit cell with the following parameters: $a = 13.704(2)$, $b = 22.329(3)$ and $c = 5.0682(8)$ Å.[6] Moreover, parameters *a* and *b* are identical to those of NON, EUO, and NES, while

Table 1. Unit cell parameters for NON, EUO, NES, and ERS-10.

Zeolite	*a* [Å]	*b* [Å]	*c* [Å]
NON[a]	13.627	22.323	15.058
EUO	13.695	22.326	20.178
NES[b]	13.698	22.660	25.213
ERS-10	13.704	22.329	5.068

[a] matrix: (010, 001, 100). [b] matrix: (100, 001, 010).

[*] Dr. S. Zanardi, Prof. G. Cruciani
Sez. di Mineralogia, Petrologia e Geofisica
Dip. Scienze della Terra
Università degli Studi di Ferrara
Corso Ercole I d'Este 32, 44100 Ferrara (Italy)
Fax: (+39) 0532-210-161
E-mail: zrs@unife.it
Dr. R. Millini, Dr. L. C. Carluccio, Dr. G. Bellussi, Dr. C. Perego
EniTecnologie S.p.A.
Via F. Maritano 26, 20097 San Donato Milanese (Italy)
E-mail: rmillini@enitecnologie.eni.it

[**] The authors thank Italian CNR and MURST ("Zeolites, materials of interest for industry and environment: synthesis, crystal structure, stability and applications." COFIN 2001) for financial support.

  0044-8249/02/4121-4109 $ 20.00+.50/0

c is $^1/_4$ that of EUO, that is the thickness of the above-mentioned pseudo-hexagonal sheet. This was considered a strong indication that ERS-10 is closely related to these zeolites. Furthermore, the presence of broad reflections supported the hypothesis that ERS-10 is a disordered member of this zeolite family.

This hypothesis was further confirmed by the discovery of NU-85, recognized as an EUO/NES intergrowth.[10] The reflections that appear broad in the XRD pattern of ERS-10 are still sharp in the case of NU-85, but their relative intensity depends on the extent of the intergrowth phenomena.[10] It is therefore clear that ERS-10 and NU-85 are two disordered members of the same family of zeolites. However, instead of treating ERS-10 as an intergrowth of EUO and NES alone, we considered the possibility of including also NON. The first step of the procedure was to identify the PerBUs present in the ordered structures. We focused our attention on gottardiite, the natural counterpart of NU-87, mainly for two reasons: 1) the framework topology of this zeolite allows each PerBU to be easily isolated; 2) an accurate structural model refined from single-crystal X-ray diffraction data is available for this material.[11]

Figure 2 shows the projection of the gottardiite framework along the [100] direction; the PerBUs identified in this

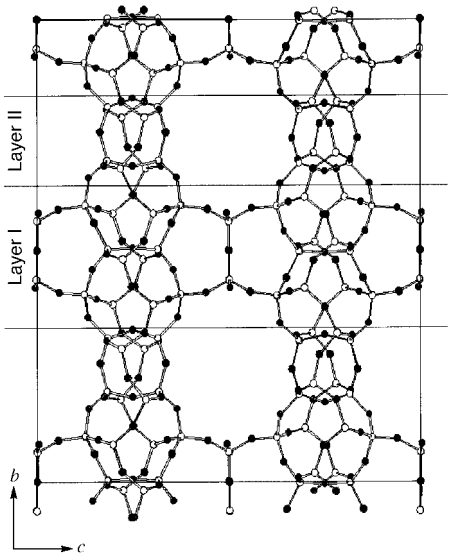

Figure 2. Framework topology of zeolite gottardiite (NES); layers I and II are also show.

structure, defined as layer I and layer II respectively, are also shown. Figure 3 shows the building scheme that allows the three framework types, NON, EUO, and NES, to be built from these layers. The DIFFaX simulations were carried out using the connection modes reported in Table 2. Several trials were performed in which different layer-to-layer stacking probabilities were adopted, and the results of each trial were evaluated by comparing the powder pattern calculated with DIFFaX with that of calcined ERS-10. A third layer (see Table 2) structurally identical to layer I was introduced to account for fault clustering. This implies that the "I to I" stacking sequence forms thick domains instead of being

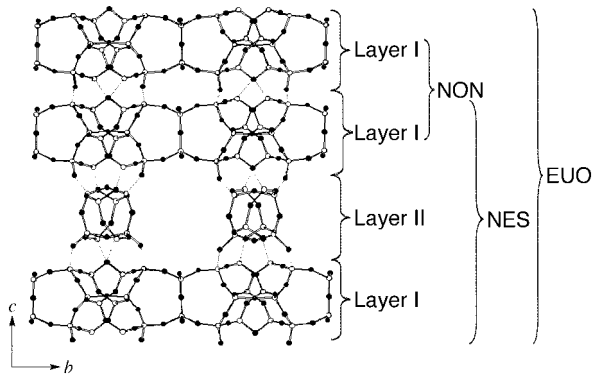

Figure 3. Building scheme of NON, EUO, and NES, starting from layers I and II (DIFFaX setting).

Table 2. Layer–layer transition adopted.

From layer	To layer	Translations	Probability first step [%]	Probability second step [%]
I	I	0.5 *a*	34	34
I	I′[a]	0.5 *a*	33	33
I	II	none	33	33
I′[a]	I	0.5 *a*	25	25
I′[a]	I′[a]	0.5 *a*	55	55
I′[a]	II	none	20	20
II	I	0.5 *a*	50	40
II	I′[a]	0.5 *a*	50	40
II	II	none	0	20

[a] Layer I′ structurally identical to layer I.

randomly dispersed throughout the crystals. For further details on the meaning of this fault clustering see the paper by Treacy et al.[4] The best agreement was found when the probabilities listed in Table 2 (first step) were used, leading to a satisfactory reproduction of the basic features of the calcined ERS-10 synchrotron powder diffraction pattern (SXPD, Figure 4). However, some minor differences between the two patterns still persist because DIFFaX is not a refinement program.

The structural model obtained so far is based on a random distribution, perpendicular to the stacking vector (the crystallographic *b* axis in the gottardiite setting, corresponding to the *c* axis in the DIFFaX setting), of straight channels with 6–

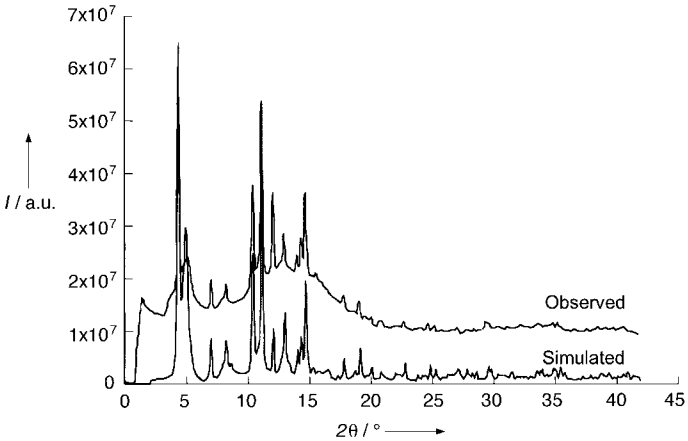

Figure 4. Comparison between the observed and the simulated SXPD patterns of ERS-10 (stacking probabilities as in Table 2, step 1).

  0044-8249/02/4121-4110 $ 20.00+.50/0 *Angew. Chem. Int. Ed.* **2002**, *41*, No. 21

and 10-ring openings (Figure 5). Moreover, adjacent one-dimensional channels are linked by short 12-ring channels or side pockets whose dimensions depend on the stacking faults; in any case the access to these bridging sections is possible only through 10-ring windows.

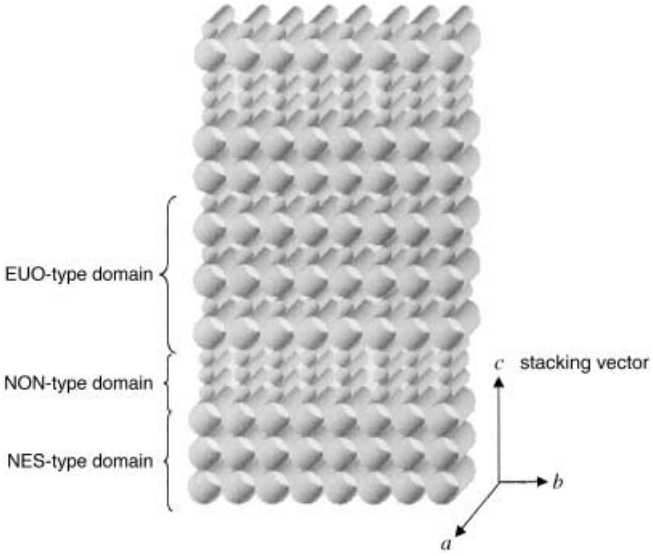

Figure 5. Roll stacking disordered model of zeolite ERS-10 (DIFFaX setting), is possible to show the random sequence of the straight 10-ring channels (large cylinders) and 6-ring ones (small cylinders).

This result is somewhat in contrast with the catalytic performances of zeolite ERS-10.[12] In particular, for ERS-10 a spaciousness index (SI)[13] of 5.3 apparently indicates a pore width close to that of offretite, a zeolite characterized by a monodimensional linear channel system with 12-ring openings.[12] Actually, an SI of 5 was reported also for the medium-pore EUO zeolite and this anomalous value was explained with the presence of the large 12-ring cavities in its porous structure.[14] Since the SI alone is not sufficient for defining the pore width of ERS-10, other test reactions, that is the ethylbenzene disproportionation and the liquid-phase alkylation of benzene with propylene, were considered, leading to the conclusion that the effective ERS-10 pore width is in the intermediate range between those of medium- and large-pore zeolites.[12]

There are two possible explanations for this. The first one implies the existence on the crystal surface of cups with 12-ring openings, corresponding to the side pockets mentioned above: a situation similar to that observed for ERB-1 (IZA code MWW).[15] This material belongs to the class of medium-pore zeolites, being characterized by the presence of two noninterconnected channel systems both with 10-ring openings; however, it displays outstanding catalytic properties typical of large-pore zeolites.[15] These features were attributed to the fact that the reaction takes place in the 12-ring cups present on the [001] crystal surface.[15]

The second possible explanation concerns the existence of very large channels with egg-shaped 14-ring openings, which can be generated when a layer II–layer II interconnection occurs (Figure 6). This situation, not considered in the first model, led to an improvement of agreement between the

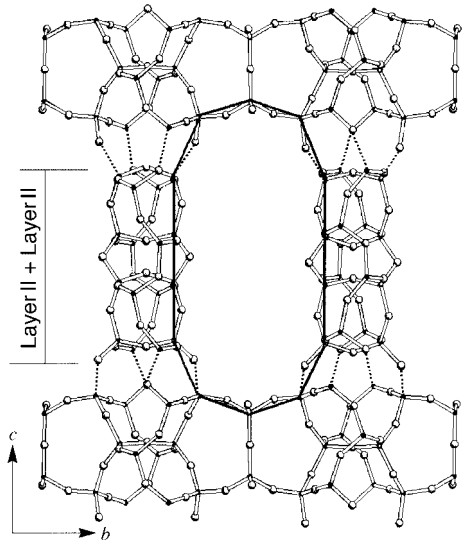

Figure 6. Egg-shaped 14-ring openings generated by the layer II–layer II interconnection (DIFFaX setting).

simulated and the experimental diffraction pattern, due to the reduced intensity of the broad reflection located at $\approx 4°$ 2θ (Figure 7). The best results were obtained when the layer II–layer II stacking probability was set to 20% (Table 2, second step).

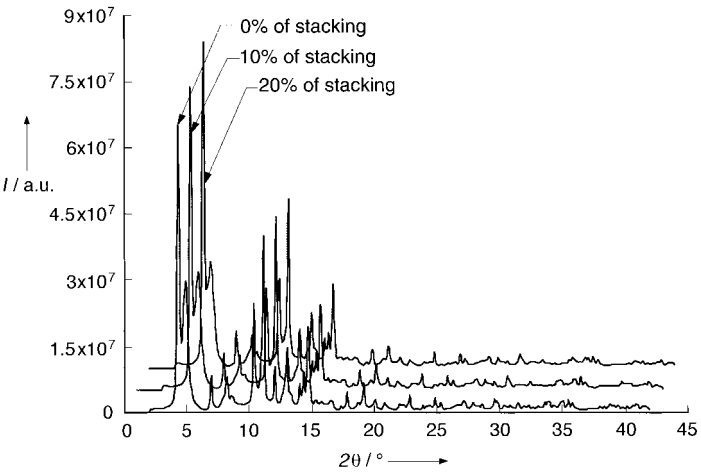

Figure 7. Simulated diffraction pattern with increasing layer II–layer II stacking probabilities.

Although the existence of 14-ring channels in ERS-10 structure remains to be confirmed by other techniques (e.g. by HREM[16]), it is clear that their presence accounts well for the catalytic performances of this zeolite.

In any case, what emerges from this work is that ERS-10 is really an intergrowth of zeolites NON, EUO, and NES, a conclusion supported by the fairly good agreement between the simulated and the experimental SXPD patterns.

Experimental Section

Synthesis: ERS-10 zeolite was synthesized according to the method reported in reference [6]. NaOH, aluminum isopropylate, and 6-azonia-spiro-[5,5]-undecane hydroxide were dissolved in demineralized water and

  0044-8249/02/4121-4111 $ 20.00+.50/0

the resulting solution was heated at 353 K. The silica source (tetraethylorthosilicate, TEOS) was added gradually under vigorous stirring, then the resulting mixture was aged for 4 h, cooled to room temperature, charged in an oscillating stainless-steel autoclave and heated at 443 K for 336 h. After crystallization the autoclave was cooled to room temperature with cold water. The solid product was collected by filtration, repeatedly washed with demineralized water, and finally dried overnight at 423 K. A fraction of the solid was calcined at 823 K for 4 h to remove the organic molecules trapped in the ERS-10 pores.

Powder data collection: X-ray powder diffraction (XRD) patterns were obtained with a Philips X'PERT diffractometer equipped with a pulse-height analyzer and a secondary curved graphite crystal monochromator. Data were collected stepwise over $3 \leq 2\theta \leq 53°$, with a step size of $0.02° 2\theta$ and an accumulation time of 20 s per step, using $Cu_{K\alpha}$ radiation ($\lambda =$ 1.54178 Å).

Synchrotron X-ray powder diffraction data were collected at room temperature on a sample loaded in a glass capillary mounted in Debye–Scherrer geometry at BM08, GILDA beamline (ESRF, Grenoble) during the experiment 08-02-174. The beamline was set to deliver a wavelength of $\lambda = 0.82714$ Å, and the data was collected on a Fuji Image Plate located at 204.83 mm from the sample and perpendicular to the incident beam; the exposure time was 3 min. Elaboration of the scanned digital images (Fuji BAS2000 scanner) was carried out using the Fit2d software package.[17]

Received: June 25, 2002 [Z19608]

[1] G. Perego, M. Cesari, G. Allegra, *J. Appl. Crystallogr.* **1984**, *17*, 403.
[2] J. M. Newsam, M. M. J. Treacy, W. T. Koetsier, C. B. De Gruyter, *Proc. R. Soc. London Ser. A* **1988**, *420*, 375.
[3] J. B. Higgins, R. B. LaPierre, J. L. Schlenker, A. C. Rohrman, J. D. Wood, G. T. Kerr, W. J. Rohrbaugh, *Zeolites* **1988**, *8*, 446.
[4] M. M. J. Treacy, J. M. Newsam, M. W. Deem, *Proc. R. Soc. London Ser. A* **1991**, *433*, 499.
[5] L. Carluccio, R. Millini, G. Bellussi Eniricerche S.p.A., European Patent 796,821 **1997**.
[6] R. Millini, L. Carluccio, F. Frigerio, W. O. Parker, Jr., G. Bellussi, *Microporous Mesoporous Mater.* **1998**, *24*, 199.
[7] N. A. Briscoe, D. W. Johnson, M. D. Shannon, G. T. Kokotailo, L. B. McCuster, *Zeolites* **1988**, *8*, 74.
[8] B. Marler, H. Gies, *Zeolites* **1995**, *15*, 517.
[9] M. D. Shannon, J. L. Cashi, P. A. Cox, S. J. Andrews, *Nature* **1991**, *353*, 417.
[10] J. L. Casci, M. D. Shannon, I. J. S. Lake, European Patent Application EP0462745 **1991**.
[11] A. Alberti, G. Vezzalini, E. Galli, S. Quartieri, *Eur. J. Mineral.* **1996**, *8*, 69.
[12] "Zeolites and Mesoporous Materials at the Dawn of the 21st Century": C. Perego, M. Margotti, L. Carluccio, L. Zanibelli, G. Bellussi, *Stud. Surf. Sci. Catal.* **2001**, *135*, 178.
[13] "Zeolites: Facts, Figures, Future": J. Weitkamp, S. Ernst, C. Y. Chen, *Stud. Surf. Sci. Catal.* **1989**, *49*, 1115.
[14] "Innovation in Zeolite Materials Science": R. Kumar, S. Ernst, G. T. Kokotailo, J. Weitkamp, *Stud. Surf. Sci. Catal.* **1988**, *37*, 451.
[15] C. Perego, S. Amarilli, R. Millini, G. Bellussi, G. Girotti, G. Terzoni, *Microporous Mater.* **1996**, *6*, 395.
[16] HRTEM analyses on ERS-10 were unfortunately unsuccessful primarily for two reasons: 1) the extremely low stability of the crystallites under the electron beam (they undergo amorphization immediately, independently of the conditions adopted); 2) the unfavorable morphology of ERS-10, which crystallizes in the form of relatively compact agglomerates of small crystallites, difficult to separate.
[17] A. P. Hammerslay, S. O. Svensson, M. Hanfland, A. N. Fitch, D. Häusermann, *High Pressure Res.* **1996**, *14*, 235.

Direct Electrophilic Insertion into a Twelve-Vertex Metallacarborane**

Alexander R. Kudinov,* Dmitry S. Perekalin, Stanislav S. Rynin, Konstantin A. Lyssenko, Gennadii V. Grintselev-Knyazev, and Pavel V. Petrovskii

In memory of Margarita I. Rybinskaya

Direct insertion of metal-complex fragments into *closo*-carboranes and metallacarboranes to give polyhedral expansion products is one of the most interesting reactions in metallacarborane chemistry.[1] The nucleophilic insertion into the cage molecules has been well studied.[2] Herein we report the first direct electrophilic insertion[3] into a 12-vertex metallacarborane.

We studied the reaction of ruthenacarborane anion **1** with $[(\eta\text{-}C_5R_5)Ru(MeCN)_3]^+$ (R = H, Me) (Scheme 1). The electrophilic attack of the fragments $[(\eta\text{-}C_5R_5)Ru]^+$ was expected

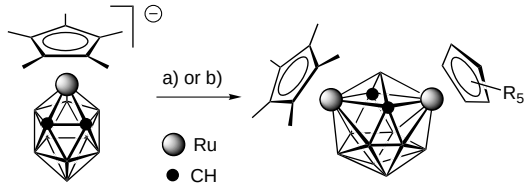

$[(\eta\text{-}C_5Me_5)Ru(C_2B_9H_{11})]^-$ **1**

$[(\eta\text{-}C_5Me_5)Ru(C_2B_9H_{11})Ru(\eta\text{-}C_5R_5)]$ **2a**: R = H, **2b**: R = Me

Scheme 1. Electrophilic insertion into **1** to give **2a**,**b**. Reagents and conditions: a) $[(\eta\text{-}C_5R_5)Ru(MeCN)_3]X$ (X = PF_6 or CF_3SO_3), CH_3NO_2, 100 °C, 4 h, about 50 % yield; b) $[\{(\eta\text{-}C_5Me_5)RuCl\}_4]$, THF, 20 °C or even −78 °C, 74 % yield.

to proceed at the C_5Me_5 ring to give triple-decker complexes $[(\eta\text{-}C_5R_5)Ru(\mu\text{-}\eta\text{:}\eta\text{-}C_5Me_5)Ru(C_2B_9H_{11})]$, similar to the formation of $[(\eta\text{-}C_5R_5)Ru(\mu\text{-}\eta\text{:}\eta\text{-}C_5Me_5)Ru(\eta\text{-}C_5Me_5)]^+$ by reaction of the same fragments with $[(\eta\text{-}C_5Me_5)_2Ru]$.[4] However, electrophilic insertion into the ruthenacarborane cage occurs instead to give 13-vertex diruthenacarboranes **2a**,**b**.

It should be emphasized that the electrophilic insertion reactions were previously unknown. Parent *ortho*-carborane $C_2B_{10}H_{12}$ as well as neutral metallacarboranes $[(\eta\text{-}C_5H_5)Co(C_2B_9H_{11})]$ and $[(\eta\text{-}C_5Me_5)Rh(C_2B_9H_{11})]$ were proved to be unreactive towards $[(\eta\text{-}C_5R_5)Ru]^+$. In contrast, in the case of **1** the insertion can be carried out even at −78 °C by reaction of Tl-**1** with $[\{(\eta\text{-}C_5Me_5)RuCl\}_4]$ (**3**) in THF. The high reactivity of anion **1** is evidently connected with its greater nucleophilicity.

[*] Dr. A. R. Kudinov, D. S. Perekalin, S. S. Rynin, Dr. K. A. Lyssenko, G. V. Grintselev-Knyazev, Dr. P. V. Petrovskii
Nesmeyanov Institute of Organoelement Compounds
Russian Academy of Sciences
28 ul. Vavilova, 119991 Moscow GSP-1 (Russia)
Fax: (+7) 095-135-5085
E-mail: arkudinov@ineos.ac.ru.

[**] This work was supported by the Russian Foundation for Basic Research (Grant No. 00-03-32807).

  0044-8249/02/4121-4112 $ 20.00+.50/0